

## Article

# Energy Losses or Savings Due to Air Infiltration and Envelope Sealing Costs in the Passivhaus Standard: A Review on the Mediterranean Coast

Víctor Echarri-Iribarren <sup>1,2,\*</sup> , Ricardo Gómez-Val <sup>1</sup>  and Iñigo Ugalde-Blázquez <sup>1</sup> 

<sup>1</sup> Department of Architecture, International University of Catalunya, Carrer Iradier 22, 08017 Barcelona, Spain; rjgomez@uic.es (R.G.-V.); iugalde@uic.es (I.U.-B.)

<sup>2</sup> Department of Building Construction, University of Alicante, Carretera de San Vicente s/n, San Vicente del Raspeig, 03690 Alicante, Spain

\* Correspondence: vecharri@uic.es; Tel.: +34-93-254-18-00

**Abstract:** To obtain the Passivhaus Certificate or Passivhaus Standard (PHS), requirements regarding building envelope air tightness must be met: according to the  $n_{50}$  parameter, at a pressure of 50 Pa, air leakage must be below 0.6 air changes per hour (ACH). This condition is verified by following the blower door test protocol and is regulated by the ISO 9972 standard, or UNE-EN-13829. Some construction techniques make it easier to comply with these regulations, and in most cases, construction joints and material joints must be sealed in a complex way, both on façades and roofs and at ground contact points. Performing rigorous quality control of these processes during the construction phase allows achieving a value below 0.6 ACH and obtaining the PHS certification. Yet, the value can increase substantially with the passage of time: as windows and doors are used, opened, or closed; as envelope materials expand; with humidity; etc. This could result in significant energy consumption increases and losing the PHS when selling the house at a later point in time. It is therefore important to carefully supervise the quality of the construction and its execution. In this study, we focused on a house located in Sitges (Barcelona). The envelope air tightness quality was measured during four construction phases, together with the sealing of the joints and service ducts. The blower door test was performed in each phase, and the  $n_{50}$  value obtained decreased each time. The execution costs of each phase were also determined, as were the investment amortisation rates based on the consequent annual energy demand reductions. Air infiltration dropped by 43.81%, with the final  $n_{50}$  value resulting in 0.59 ACH. However, the execution costs—EUR 3827—were high compared to the energy savings made, and the investment amortisation period rose to a 15- to 30-year range. To conclude, these airtightness improvements are necessary in cold continental climates but are not applicable on the Spanish Mediterranean coast.

**Keywords:** Passivhaus Standard; airtightness; energy efficiency; building overheating; construction quality; investment amortization; air infiltration; blower door test; envelope sealing; Mediterranean climate



**Citation:** Echarri-Iribarren, V.; Gómez-Val, R.; Ugalde-Blázquez, I. Energy Losses or Savings Due to Air Infiltration and Envelope Sealing Costs in the Passivhaus Standard: A Review on the Mediterranean Coast. *Buildings* **2024**, *14*, 2158. <https://doi.org/10.3390/buildings14072158>

Academic Editors: Alberto Meiss and Irene Poza Casado

Received: 18 May 2024

Revised: 15 June 2024

Accepted: 18 June 2024

Published: 13 July 2024



**Copyright:** © 2024 by the authors. Licensee MDPI, Basel, Switzerland. This article is an open access article distributed under the terms and conditions of the Creative Commons Attribution (CC BY) license (<https://creativecommons.org/licenses/by/4.0/>).

## 1. Introduction

According to EUROSTAT's latest available publication, the real estate sector, especially the residential sector, is responsible for 27.9% of energy consumption. This is why it is necessary to reduce the energy consumption of buildings. It is also a regulatory obligation [1]. In recent years, the European Commission has issued a number of directives to reduce energy consumption in housing construction [2,3]. These directives have been transposed into various member countries' regulatory frameworks, including in southern Europe. However, in southern European countries, a shift of mindset needs to occur towards designing more energy-efficient homes [4]. These changes have already been introduced in Spain at the regulatory level in the country's Technical Building Code (CTE), which encompasses all applicable construction regulations and includes energy consumption reduction

as an essential parameter [5–7]. Passivhaus certification (PHS) is set to gain ground as a housing construction option, owing mainly to the low operational energy consumption of Passivhaus buildings [8]. The certification requires that newly built homes follow an envelope airtightness standard below 0.6 ACH at 50 pascals (Pa) of pressure ( $n_{50}$ ). This requirement entails additional efforts for construction companies and property developers, as they need to implement a series of controls and repairs until the  $n_{50}$  requirement is fulfilled, making it possible to obtain PHS certification.

In recent years, several studies have been conducted on the performance of these buildings in terms of comfort [9] and energy efficiency. A substantial number of detailed analyses have been conducted on the functioning of these homes in cold climates, both in public buildings [10] and in private ones [11]. These analyses have demonstrated that energy consumption related to heating uses represents more than 50% in several Western countries. Optimal results have been obtained regarding the climatic behaviour of the houses studied. For example, the geometry of the façades helps to minimise the overheating of housing, such as the 115° inclination of the south façades in London [12]. The cost of incorporating the Passivhaus standard into buildings varies between 8% and 15% [13]. There have also been related studies in Mediterranean climate conditions showing that comfort requirements account for 72% of the total energy use [14], as is the case in other warm climates [15]. In this case, no unanimous results or conclusions have been reached, generating debates in the scientific community about the suitability of the PH Standard and the need to adapt it [16]. This aspect depends very much on the location. For example, in Ireland, the simulation estimated an overheating rate of 0%. The main problem detected in the research is the risk of overheating in buildings [17,18]. To this end, building shapes have been examined, as well as sun protection features and the dimensions of the openings [19], leading to an optimal window-to-façade ratio of 30%. Building shapes and distribution plans are also directly related to climatic behaviour, with an ideal ratio of 1:1.44 [20]. Analyses have even been conducted on the types of rooms in which the greatest overheating occurs, with bedrooms presenting the highest risks [21]. For all these reasons, the human factor has proven to have a direct impact on the risk of overheating in these homes, with confirmation from more than 20% of the inhabitants [22]. To improve this aspect in Passivhaus buildings, it is necessary to adopt solutions that incorporate passive natural ventilation and sunlight systems [23]. These conditions are especially suitable for warm or temperate climates, in which the architectural characteristics of the building directly influence how these buildings will function climatically in the most adverse summer months [24].

Another interesting dimension of analysis and improvement regarding Passivhaus houses is the increase in air infiltration through envelopes. It is important to observe how this latter parameter evolves by taking measurements in Passivhaus homes that have been in use for a long period of time. In this regard, it is notable that, due to the increase in recent years in the size of building openings, infiltration studies of existing buildings have detected lower air infiltration rates in older and less insulated buildings than in more modern buildings. With respect to the measurements conducted through case studies over a long period of time, such as a full year, optimistic estimates of previous energy demand simulations have been compared with actual consumption [25,26]. The real data obtained after the Passivhaus building is in operation has been shown to present higher values than those estimated through simulation.

To date, studies have focused on indoor air quality [27] and on how to improve indoor air quality and performance [28]. The ventilation demand also influences thermal comfort, resulting in an optimal relationship between a mix of natural and mechanical ventilation during 82% of the annual occupancy [29]. The interior comfort parameter is regarded as key, given that it is among the objectives of a range of current regulations. It has been found that this objective is not always met and that the measures implemented to improve comfort and indoor air quality are in fact doing the opposite. Despite comfort improvements observed in most modern buildings, which have even obtained a Passivhaus (PHS)-type

certification, it is necessary to ask whether the required efforts of Passivhaus compliance do have an effective impact on the parameters [30]. Studies have concluded that nZEBs are more likely to overheat than older and conventional buildings. These different kinds of buildings even maintain similar CO<sub>2</sub> concentrations.

In relation to air infiltration through windows, various analyses have been conducted to improve airtightness [31,32]. However, it has been shown that studies are lacking on how to homogenise the controls that allow for evaluating Passivhaus house behaviour and their operation over time [33,34]. It is particularly important to evaluate the extra cost of obtaining the PHS in hot and temperate climates, although it has been shown to perform well regarding energy demands and CO<sub>2</sub> emissions [11].

Yet, no studies have been found on both the technical and financial costs of the leak checks that must be performed in succession using the blower door test until fulfilling the Passivhaus standard requirement. For its part, the financial effort required to obtain PHS certification has been evaluated. Taking into account the various current administrative subsidies [35] and construction cost increases, it has been found to amount to approximately 30%. This extra cost is amortised over an average period of around 10 years, so the extra effort is generally considered acceptable. However, if such solutions and certifications are to be globally implemented within the country—and not restricted to luxury housing—the focus must be on low-cost or social housing scenarios [36]. Affordable social housing construction costs can be reduced by up to 22% of the build cost, even while maintaining the PHS. No studies have been performed on the additional costs and time required to achieve an  $n_{50}$  parameter below 0.6 ACH once optimal climate conditioning solutions have been applied. It is worth noting that to comply with the certification procedure, the leak detection procedure and sealing need to be performed repeatedly until fulfilling the PHS certification requirement. The punctual air infiltrations detected have a major impact on the building's overall tightness and, therefore, on its climatic conditioning and energy demands. These infiltrations usually occur through the window joinery [37]. In Passivhaus homes, these leaks are reduced to a minimum, unlike in traditional construction [38]. In the case of existing buildings, the PHS requirement of  $n_{50}$  is not as demanding as it is below 1 ACH. Despite this, the difficulty of achieving this parameter in these constructions makes such renovations even more costly, and it is not certain that the outcome will be successful [39].

Regarding home construction systems, few studies have applied modular prefabricated systems. In theory, these systems are ideal for building Passivhaus homes, but they must be optimised to ensure adequate climatic operation as well as easy and effective joint sealing produced by the system [40]. In this study, just four connection details fulfil the PHS requirements.

The Passivhaus certification requires the commitment of all agents involved, including in the design phase, the project technical drafting process, all construction phases, and subsequent use and maintenance. Insufficient production and management of these measures, commitment, and system knowledge would seriously jeopardise the expected beneficial results or lead to unforeseen negative outcomes [41]. The present work is an in-depth study of the latest requirements necessary to obtain the Passivhaus certification for a home. It highlights the measurements and work evaluation necessary to guarantee adequate envelope airtightness and the obtention of the certification, as well as the investment amortisation periods within the framework of the Mediterranean climate. A comparison with cold Central European climates is also provided.

This study's objective was to quantify the energy savings achieved during the various phases of the Passivhaus home envelope sealing and analyse the subsequent cost-effectiveness. The aim was to analyse the standard's applicability to homes located on the Spanish Mediterranean coast and to conduct a comparison with the Central European continental climate. To do this, we performed a case study analysis.

## 2. Description of the Case Study

The property under study was a newly built detached single-family house located in the municipality of Sitges (on street 30–32 Camí del Coll) in the province of Barcelona. The house has a basement, a ground floor, and a first floor (Figure 1). The basement was built with a perimeter wall and a reinforced concrete slab. The upper floors were constructed using a system of prefabricated panels made by the Evowall company. Their system of massive panels with a metal lattice was approved by the European Technical Assessment. The panels are made of a metal framework of S275 hot-rolled steel, with 5 cm of EPS thermal insulation, 8 cm of PIR thermal insulation, a mortar coating using a mixture of cement and EPS insulation, and gypsum on the inner face. The outer face consists of a mortar coating applied with a cement and insulation mix, finished with a lime mortar layer (Figure 2). The windows are made of PVC with rolling shutters. According to tests conducted by the Technological Institute of Construction (ITEC), the U of the façade panels is  $0.214 \text{ W}/(\text{m}^2 \text{ K})$ , and that of the roof panels is  $0.475 \text{ W}/(\text{m}^2 \text{ K})$ . The exterior carpentry—profiles, tracks, and shutters—was made by the Weru group.

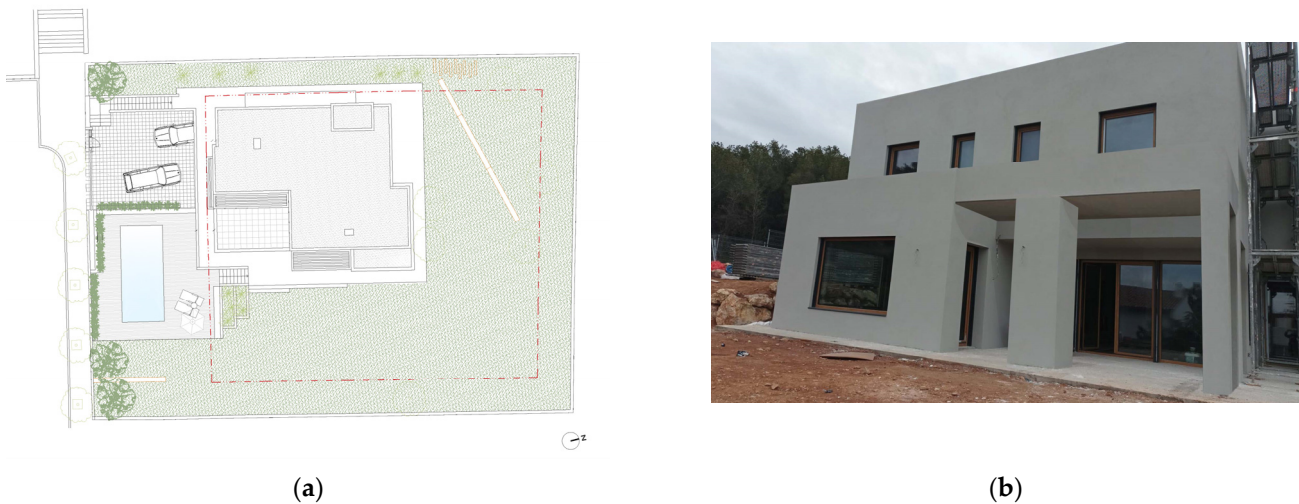


Figure 1. (a) Floor plan with dimensions; (b) Exterior view of south façade.

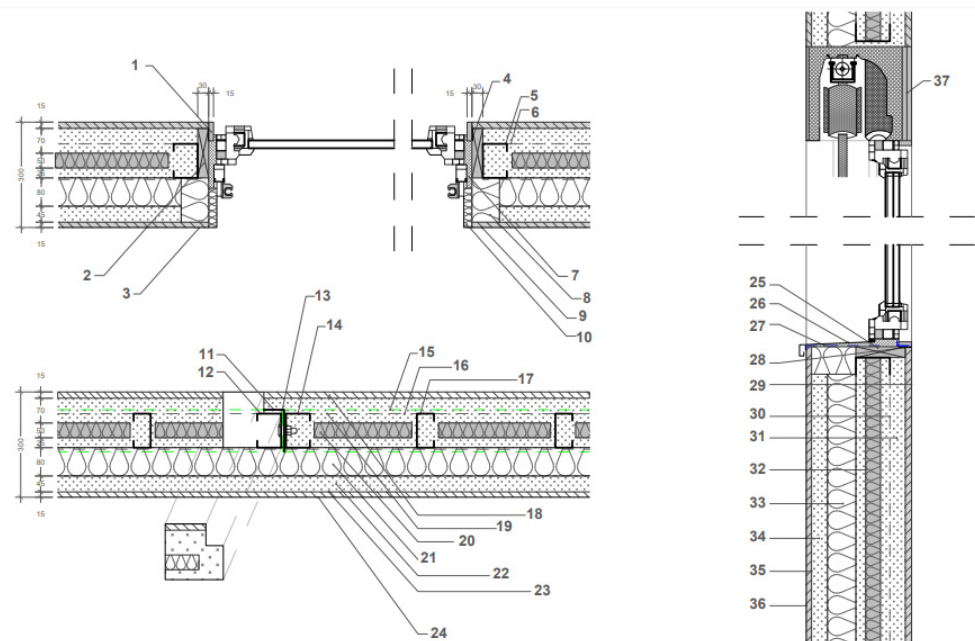


Figure 2. Cont.

Legend	
1 Plasterboard cover-piece	19 95mm Evoiin mortar
2 ISOTOP Thermapor Window Pre-frame 145x30	20 50mm EPS insulation
3 Façade finishing layer Weber system, waterproof	21 80mm PIR insulation board
4 Paint-on airtightness membrane	22 45mm Evoiin mortar
5 Steel "B" profile	23 15mm ground calcium (GCaI) mortar
6 Steel "C" profile	24 Façade finish layer/battered plaster
7 Expanding polyurethane foam	25 Expanding polyurethane foam
8 EPS insulation board, grey, 80x125mm	26 Steel cover frame
9 Mesh corner profile	27 EPDM membrane
10 EPS cover-piece 20x100mm	28 Paint-on airhightness membrane
11 Steel profile (UF)	29 15mm Plaster
12 Steel "C" profile 105x75 (UM)	30 Steel "M" profile
13 Hexagonal head bolt 8.8. Full thread DIN 933 (M16)	31 95mm Evoiin mortar
14 Connectors for panels aligned with hex. head bolt	32 50mm EPS insulation
15 Guide 120x30 (G)	33 80mm PIR insulation board
16 Inferior channel 105x50 (C)	34 45mm Evoiin mortar
17 Steel "C" profile 105x50	35 15mm Ground calcium carbonate (GCaI) mortar
18 15mm Plaster	36 Façade finishing layer Weber system Waterproof

**Figure 2.** Construction details of the typical envelopes.

This house was built in view of achieving the Passivhaus certification, which sets an  $n_{50} < 0.6$  ACH for newly-built single-family homes. The building section for which the PHS certification studies were conducted was the housing area itself, located on the ground floor and the first floor (Figure 3). The garage and the machine room in the basement were, therefore, not built according to Passivhaus standards.

The layout is shown in Figure 4. To ensure appropriate sealing and to comply with the PHS requirements, different measurements were taken by the construction company using the blower door test. Measurements were taken by the construction company on several occasions, specifically on 3 October 2023 and 21 November 2023. On 5 December 2023, the Praxis company, specialising in Passivhaus certification, was required to perform the blower door test. Measurements were also made using a digital anemometer and smoke machine to detect air leaks during these tests.



**Figure 3.** Cont.

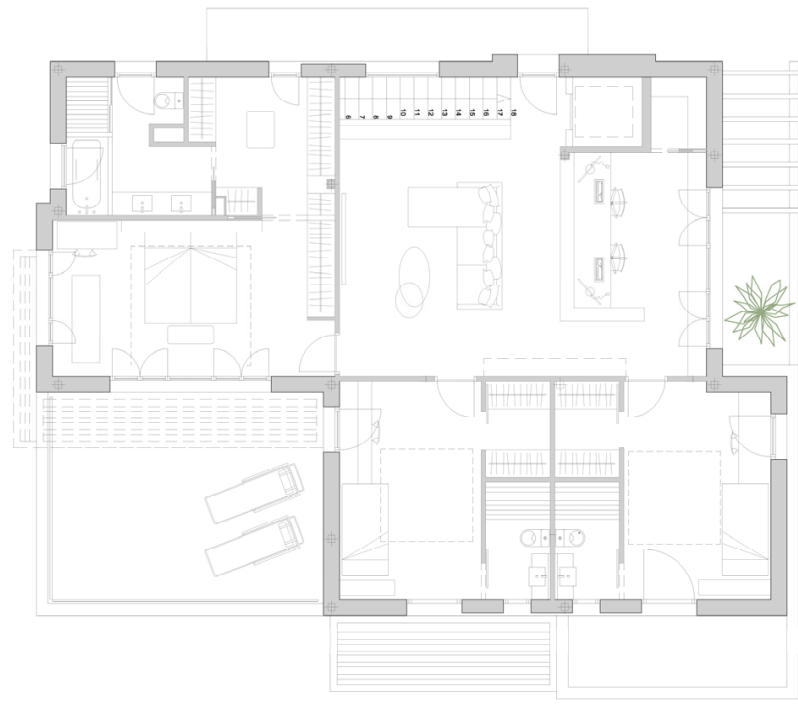


**Figure 3.** Furnished and delimited ground floor and first floor.

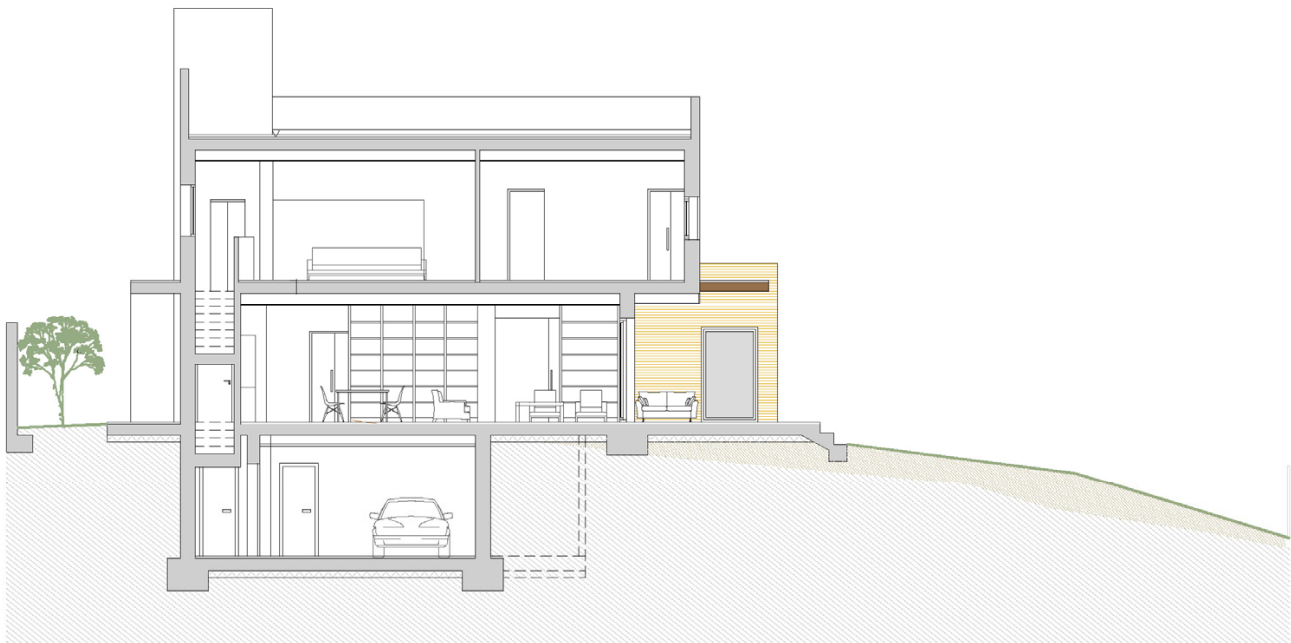


**Figure 4.** Cross-section of the kitchen and first-floor master bedroom.

The conducted tests led the construction company to carry out a series of additional seals, especially in the service ducts, which presented the greatest number of detected air leaks (Figure 5). Plastic tape and elastic amorphous seals were used for the sealing.



**Figure 5.** (a) Detection of air infiltration after phase P1; (b) Details of sealing using adhesive tape.

### 3. Materials and Methods

A building's annual energy demand depends on various factors, some of which are highly complex, such as the orientation, local climate, materials used, and the technical characteristics of the envelopes [42]. Assessing the actual heat flow through envelopes over the cycle of a week, a month, or a full year is a truly complex task [43]. It requires simulation tools that consider the envelope thermal inertia and ground contact, the thermal bridges of the construction systems used, as well as the solar radiation on the exterior surfaces or the air conditioning systems used. In addition, factors relating to the construction's inherent deficiencies must be considered, such as contacts between different materials, joineries, intrinsic humidity variations, expansion effects during the material execution of the project, etc. Envelope airtightness varies according to climatic conditions, outside air pressure at any given time, and the maintenance and usage by the home's users of mobile elements such as carpentry, adjustable slats, or grids [44]. This makes it difficult to estimate or quantify the real energy impact of air infiltration, which is also subject to unforeseen events and imbalances. Constant variations in outdoor air pressure make it even harder, although this point can be solved by obtaining annual statistical averages per season or at specific times of the year [45]. Despite the above, designing a suitable methodology and strategy to extract data from methodology-adapted parameters allows for approaching the problem with the necessary level of quality assurance.

#### 3.1. Envelope Airtightness

The main study objective was to quantify the energy impacts of envelope airtightness under various scenarios and to estimate the corresponding investment amortisation. To this end, we present below the case study of a house whose envelope airtightness value was

expected to be low owing to the quality of the construction company and the prefabrication system used, as well as the applied sealing, carpentry quality, and air tightness.

The execution of the envelope sealing took place over four phases at four- and six-week intervals. We performed the blower door test four times, immediately after each phase. This allowed for making on-site decisions regarding the technique to be used in phases P2, P3, and P4, and whether or not to carry them out. This was performed according to the  $n_{50}$  value obtained, the expected execution costs for each phase, and the amortisation of these seals according to the energy savings made.

#### Phase P1

Sealing of construction joints using a hermetic liquid membrane. Application of expanding polyurethane foam in joinery together with the façade envelope manufacturers. Plastic adhesive tape and amorphous seals. Completed in September 2023.

#### Phase P2

Detection of critical points. Sealing of joints of materials and plane contacts using polyurethane expanding foam. Contact between carpentry and shutter units with ISO3 polyurethane-based adhesive plastic tapes. Amorphous seals.

#### Phase P3

Sealing of joints between plane contacts and materials using polyurethane expanding foam. Seals in installation passageways, mainly electrical ones, are based on ISO3 polyurethane-based adhesive plastic tapes and elastic amorphous ISO-TOP seals.

#### Phase P4

Detection of insufficiently airtight spots. Joints are sealed using techniques similar to those in P3.

To evaluate the envelope airtightness value, the blower door test was conducted in the various construction phases. It was executed in accordance with European Standard EN 13829 (Thermal performance of buildings—Determination of air permeability of buildings—Fan pressurization method) using the blower door GMBH MessSysteme für Luftdichtheit equipment. Corresponding graphs were obtained for pressurisation and depressurisation at 10–70 pascals (Pa) of air pressure and an  $n_{50}$  airtightness value of 50 Pa. A specific sheet developed for the research group “Architecture & Energy” of the University of Valladolid was used to characterise the resulting information [46]. This tool was developed specifically to characterise 140 parameters that can intervene in infiltration [46]. The parameters were collected in a database, which was then used for the overall result evaluation.

To obtain the average building envelope airtightness value—a parameter that is always difficult to quantify—we followed the protocol established in the UNE-EN-ISO 13790:2008 standard. This method allows for converting the  $n_{50}$  value to a rate of changes/hour under normal pressure conditions and as an average value over a time interval via the following expression:

$$n_{winter} = 2 \cdot n_{50} \cdot e_i \cdot \varepsilon_i, \quad (1)$$

$n_{50}$ —air changes/hour at 50 Pascals;

$e_i$ —wind protection coefficient = 0.05;

$\varepsilon_i$ —height correction factor = 1.

In this way, using the DesignBuilder version 7 tool and the mathematical corpus described in Section 3.2.1, it was possible to simulate the energy impact. We obtained global annual energy demand values and partial ones exclusively due to the envelope airtightness value.

We used the blower door test tool to detect thermal bridges through images from Flyr’s ThermaCam P25 thermal imaging camera. The quantification was conducted using the AnTherm programme, and we estimated a thermal bridge gain or loss of pressure of 3.5% of the total thermal loads due to the envelope thermal transmittance U-values, which were close to those obtained in previous studies [47,48].



### 3.2. Assessment of the Energy Impact of Air Infiltration

Estimating the energy impact of air infiltration is an arduous task. It cannot be entirely accurate, as it depends not only on the airtightness of the building envelope but also on weather conditions, which are usually difficult to predict [49]. No common criterion exists regarding which model is suitable to assess the energy impact of air infiltration through the envelope [50]. So far, different calculation models have been developed to varying degrees of complexity and reliability [51]. The simplest models are based on a uniform distribution of leak pathways and constant average leaks over time. In this study, the impact was evaluated using two different tools and methodologies: a simplified calculation model (Equations (1)–(8)), and DesignBuilder simulation software.

#### 3.2.1. Application of the Simplified Calculation Model

The first simplified calculation model used applies the degree-day concept, which links the average temperature outside the tested home to the indoor comfort temperature (21 °C for heating and 24 °C for cooling) [7]. This estimate is theoretical: real energy consumption depends on each household's specific indoor air temperature  $T_i$  setpoint conditions. This calculation procedure makes it possible to assess the  $Q_{inf}$  energy impact considering specific climatic data of the house location. The calculation considers the air infiltration flow obtained through the blower door test  $n_{50}$ , the specific capacity of the  $V_{inf}$  air in the area under study, and the temperature differences between the home's indoor air  $T_i$  and outdoor air  $T_e$  [52].

$$Q_{inf} = C_p \cdot G_t \cdot V_{inf}, \quad (2)$$

Here,

$Q_{inf}$  is the annual energy loss (kWh/year) due to air infiltration.  $Q_{inf-H}$  is considered for heating and  $Q_{inf-C}$  for cooling. Annual energy losses are expressed per surface area unit.

$C_p$  is the specific air heat capacity, which is 0,34 Wh/m<sup>3</sup>K.

$G_t$  is the number of annual degree-days (kKh/year), both for heating ( $G_{t-C}$ ), with a basic comfort temperature of 21 °C, and for cooling ( $G_{t-R}$ ), with a basic comfort temperature of 25 °C.

$V_{inf}$  is the air leakage rate (m<sup>3</sup>/h).  $V_{inf}$  must be obtained from the values obtained in the test, which are expressed with a pressure difference of 50 Pa and do not reflect the actual filtration process to which the house is subjected.

The Persily–Kronvall estimation (Equation (3)) is a simple and widespread model in the scientific community, and it was adopted in this first model [53]. It assumes a linear relationship between permeability at 50 Pa and the average annual infiltration:

$$q_{inf} = q_{50} / 20, \quad (3)$$

where

$q_{inf}$  is the air permeability (m<sup>3</sup>/(h m<sup>2</sup>)).

$q_{50}$  is the air permeability at 50 Pa (m<sup>3</sup>/(h m<sup>2</sup>)).

This linear relationship between tightness and infiltration was subsequently evolved [53], incorporating some parameters and coefficients based on the house location characteristics according to Equations (4) and (5):

$$q_{inf} = q_{50} / N, \quad (4)$$

$$N = C \cdot cf_1 \cdot cf_2 \cdot cf_3, \quad (5)$$

where

$N$  is a constant.

$C$  is the climate factor, calculated in the model using hourly climate data for over 200 points in the U.S. and Canada. The value ranges from 15 to 30.

$cf_1$  is the building height correction factor, applicable to buildings in which the tested spaces are on one floor ( $cf_1 = 1$ ) up to three floors ( $cf_1 = 0.7$ ).

$cf_2$  is the site shielding correction factor, for well-shielded cases ( $cf_2 = 1,2$ ), ( $cf_2 = 1$ ) or exposed houses ( $cf_2 = 1$ ), ( $cf_2 = 0.9$ ).

$cf_3$  is the leak correction factor, which depends on the value of the leakage exponent  $n$ . Buildings with small cracks receive a correction factor  $cf_3 = 1.4$  while leaking buildings with large cracks or holes have a correction factor  $cf_3 = 0.7$ .

This extended simplified model was adopted to calculate the average infiltration flow in the Spanish Mediterranean region, obtaining the climatic factor  $C$  value through assimilation with US climates as a function of the average temperature and wind speed. For the coefficients  $cf_1$ ,  $cf_2$ , and  $cf_3$ , a value equal to 1 was adopted in all three cases, since the small cracks detected in the envelope of the dwelling reached an average value. The type of infiltration opening was obtained from the mean value of the flow exponent,  $n = 0.59$ . The  $V_{inf}$ , or air leakage rate, required to determine the energy impact was calculated based on the air permeability rate and the envelope surface area (Equation (6)):

$$V_{inf} = q_{inf} \cdot A_E, \quad (6)$$

where

$A_E$  is the envelope area ( $m^2$ ).

Once we obtained the value of the envelope air infiltration volume or air leakage rate  $V_{inf}$  to calculate the energy impact according to the annual average corrected through Equations (1)–(6), we quantified the sensible heat  $Q_s$  and latent heat  $Q_l$  using the following equations:

$$Q_s = V_{inf} \cdot C_e \cdot \rho \cdot (T_e - T_i), \quad (7)$$

Here,

$Q_s$  is the value of the energy impact of the sensible heat of the air leakage rate  $V_{inf}$  (W).

$V_{inf}$  is the air leakage rate ( $m^3/h$ ).

$C_e$  is the specific air heat under normal conditions (0.349 Wh/kgK).

$\rho$  is the air density ( $kg/m^3$ ).

$T_e$  is the outside air temperature in degrees Kelvin (K), taken as an annual average value.

$T_i$  is the inside air temperature (21 K in winter and 24 K in summer).

$$Q_l = V_{inf} \cdot C_v \cdot \rho \cdot (W_e - W_i), \quad (8)$$

Here,

$Q_l$  is the energy impact value of the latent heat of the air leakage rate  $V_{inf}$  (W).

$V_{inf}$  is the air leakage rate ( $m^3/h$ ).

$C_v$  is the water vaporisation heat (0.628 W/g<sub>vapour</sub>).

$\rho$  is the specific air volume ( $kg/m^3$ ).

$W_e$  is the specific outside air humidity taken as the annual average value (g<sub>vapour</sub>/kg).

$W_i$  is the specific indoor air humidity (g<sub>vapour</sub>/kg).

### 3.2.2. Obtaining Annual Energy Demand Using DesignBuilder

The second quantitative approximation method was executed through DesignBuilder. To quantify the energy impact, the U-value transmittance values of all envelopes [54] obtained in situ using the TESTO 635-2 [55,56] equipment were entered into the DesignBuilder model. To simulate the building's behaviour in terms of energy demand and interior comfort parameters, the data and parameter values described next were introduced into the tool. The winter period ran from 1 December to 30 April, and the summer period from 1 May to 30 November. This decision was based on the results obtained in previous studies and according to the various model calibrations performed in the same geographical location. The indoor air temperatures were set at 21 °C in winter and 24 °C in summer. Maintenance temperatures of 17 °C in winter and 27 °C in summer were selected for night-time. For the regulatory calculation of air renewal, the occupancy was 5 people. To comply with regulations, a value of 0.63 ACH was established according to

Spain's current Technical Building Code (CTE). The model was applied by eliminating the existing basement of the dwelling, considering a very airtight access door, and calculating the energy loss values with the  $U$ -value, as if the ground floor were in contact with the ground. The air infiltration values entered in the tool were those obtained by the blower door test. All parameters related to the outdoor climate, including the solar radiation values, setpoint temperatures, air change rate according to the CTE regulations, etc., were entered into the DesignBuilder tool. The calculation model used in DesignBuilder was that of the total demand for all energy necessary to establish the set temperature conditions. Therefore, the energy efficiency of the heat recovery unit was not taken into account. The infiltration values obtained in the  $n_{50}$  were applied in the four construction phases P1, P2, P3, and P4, with the calculated air infiltration value average of the building envelope being transformed according to expression (1).

A thermoflowmetric study of the opaque envelopes was conducted for the two south façade rooms (kitchen at a height of 0.70 m and living room), the north façade (multipurpose room), and the north and south façade first-floor bedrooms. The ground contact U-value transmittance was also calculated in accordance with ISO 9869-1:2014 [57]. The tests lasted at least one week for each U-value transmittance measurement. The data were analysed using AMR WinControl software (<https://www.ahlborm.com/en/products/amr-win-control-software-for-data-acquisition-and-measured-data-processing>) developed by Ahlborn for ALMEMO measuring equipment. The method used was the "average method", i.e., the thermal transmittance was calculated by dividing the thermal flow average density by the difference in average temperature [58,59].

### 3.3. Air Infiltration and Its Energy Impact: Investment Amortisation Approach

Having established a method to quantify the air infiltration energy impact and compare it using DesignBuilder, it was possible to pursue the study objectives. To this end, four phases of the construction and sealing process, P1, P2, P3, and P4, were technically defined, and the execution cost of each was quantified. The investment amortisation period was estimated according to the methodology shown in Figure 6.

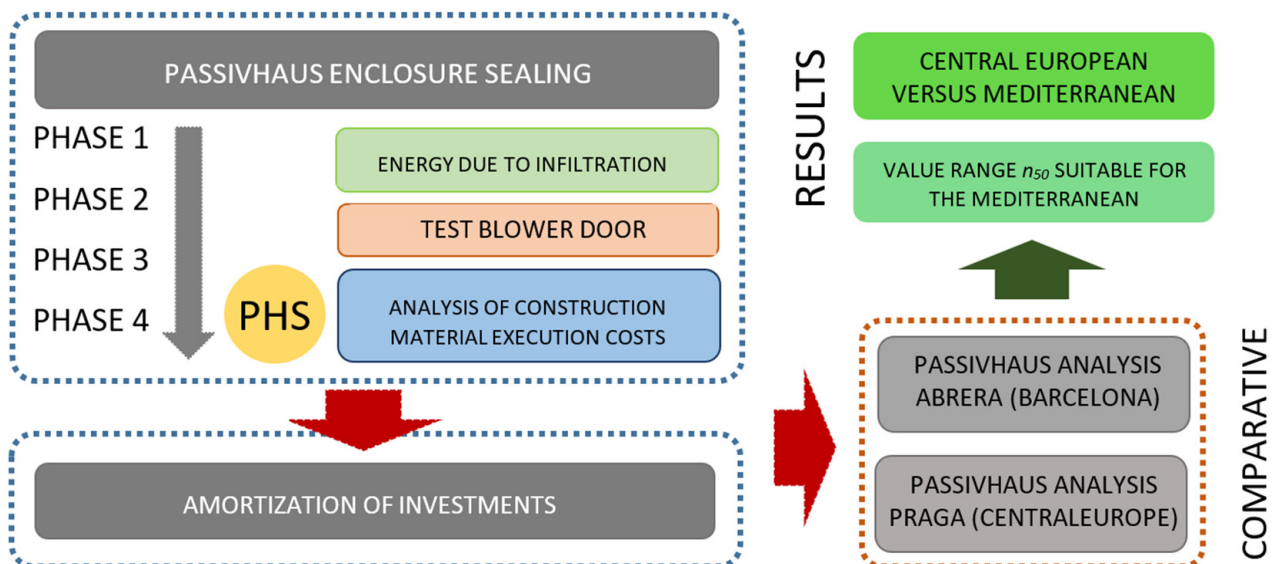


**Figure 6.** Methodology to assess energy and investment amortisation in the 4 scenarios under study.

The  $n_{50}$  value and the actual building envelope airtightness over the entire one-year cycle were progressively analysed over the 4 phases, together with the energy impact due to these air infiltrations. Finally, the home's life cycle cost (LCC) was applied in the 4 scenarios or designed phases. To this end, the UNE-EN 15459-1:2018 [60] standard was applied to

the house CCL in the 4 scenarios, P1, P2, P3, and P4. The overall cost was calculated using the following expressions:

$$C_g(t) = C_l + \sum_j \left[ \sum_{i=1}^t (C_{a,i}(j) \cdot R_{disc}(i)) - Val_{E,t}(j) \right], \quad (9)$$

$$R_R = \frac{R_{int} - R_i}{1 + R_i/100}, \quad (10)$$

$$R_{disc}(i) = \left( \frac{1}{1 + R_R/100} \right)^i, \quad (11)$$

where

$C_g$ —overall cost.

$C_l$ —initial investment costs.

$C_a$ —recurring costs.

$R_{disc}$ —discount rate.

$i$ —years.

$Val_f$ —residual value (EUR).

$R_R$ —real interest rate.

$R_i$ —inflation rate.

$R_{int}$ —interest rate.

The investment costs, recurring costs, and maintenance costs for a period of 30 years were obtained from various databases of companies in the sector in Barcelona. The costs of the energy consumed over 30 years were determined using expressions (7) and (8), adjusted to the DesignBuilder simulation estimates, and an electricity mix cost of 0.242 EUR/kWh [61].

This quantification of overall execution costs and the savings achieved by reducing the actual envelope airtightness in each phase allowed us to address the study hypothesis. By subsequently determining the market value of the Passivhaus certification and comparing it with non-certified housing values, we could establish whether it would be advisable or not to adopt the sealing requirements of phases P2, P3, and P4 to reduce the  $n_{50}$  value below 0.6 ACH.

#### 4. Results

Table 1 shows the  $n_{50}$  results obtained from the blower door test in each of the 4 phases, as well as the estimation of the energy loss calculation due to air infiltration according to expression (1). As can be observed, the initial value was above 0.6 ACH, and a substantial reduction was achieved in phases P2 (Figure 7), P3, and P4, dropping below the maximum value allowed by the Passivhaus standard. The techniques for detecting the largest infiltration points, in addition to those applied for sealing, were satisfactory, and the desired objective was met. Since similar results have been obtained in previous publications, we were able to conclude that the work was technically valid [32,37].

**Table 1.** Results of  $n_{50}$  and average winter and summer infiltration in the three phases.

Envelope Air Infiltration	$e_i$	$\epsilon i$		P1	P2	P3	P4	% Reduction
$n_{50}$ (blower door test)			ACH	1.05	0.95	0.75	0.59	43.81
$n_{winter}$ and $n_{summer}$	0.05	1	ACH	0.105	0.095	0.075	0.059	43.81

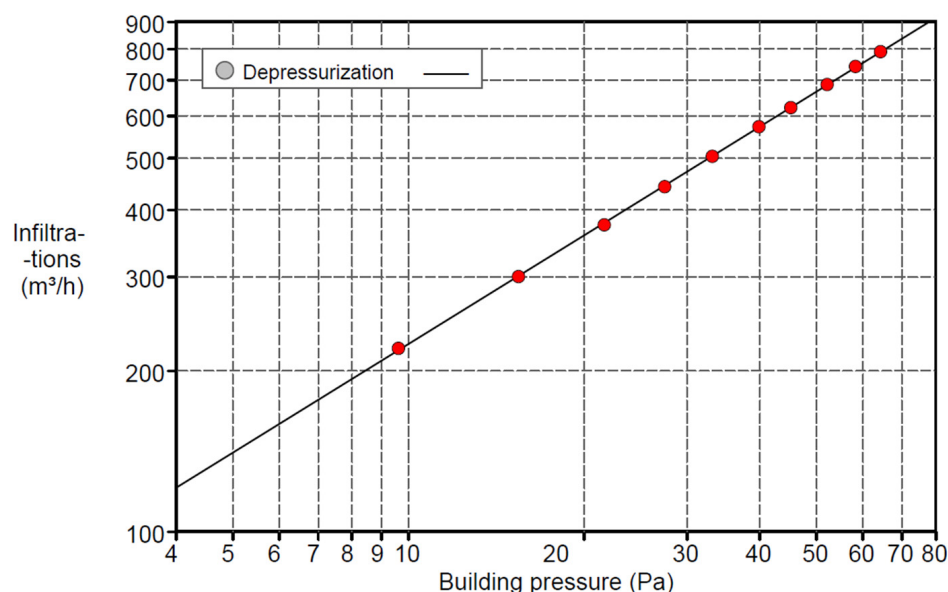


**Figure 7.** Results from  $n_{50}$  and the blower door test in phase P2.

Regarding the translation of these values into energy consumption quantifications, Table 2 breaks down the methodological process in Section 3.2.1., in which  $C = 18$ ,  $cf_1 = 1$ ,  $cf_2 = 0.9$ , and  $cf_3 = 1.4$ . This air infiltration energy demand is also given with respect to the energy demand of air changes of 0.63 ACH and the annual energy demand due to air conditioning. These values are similar to those obtained in previous publications [30]. The energy demand due to envelope air infiltration accounted for 16.41% of the annual energy demand in P1 and dropped to 11.93% in P3. These values are high for conventional homes but not for Passivhaus Certificate housing, where thermal load reduction and the heat recovery system substantially reduce annual energy demands [62].

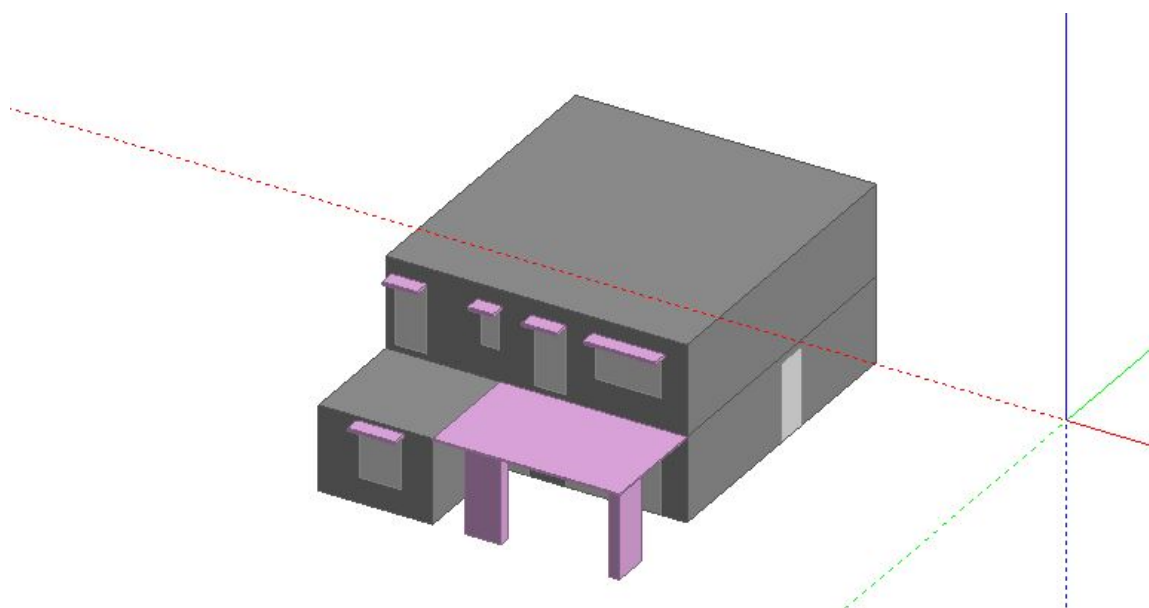
**Table 2.** Calculation of annual energy demands due to air infiltration in the four phases.

Parameter		Material Execution and Sealing Phases			
Phase		P1	P2	P3	P4
$q_{inf}$	$m^3/hm^2$	0.289	0.262	0.207	0.164
$V_{inf}$	$m^3/h$	73.87	66.97	52.79	41.92
$Q_s$	kWh/y	319.15	288.75	227.96	179.33
$Q_l$	kWh/y	2632.28	2381.58	1880.20	1479.09
Annual energy demand due to infiltration	kWh/m <sup>2</sup> y	6.55	5.74	4.46	3.73
Annual energy demand (expressions (1) to (8))	kWh/y	10,203.60	9989.37	9560.18	9191.32
Percentage %		100.00	97.79	93.69	90.08

As illustrated in Table 3, the results of the DesignBuilder simulations (Figure 8) are visibly close to those obtained through the mathematical expressions (1 to 8), with a maximum deviation of 2.2%. They were both conducted to obtain the annual energy demand. For the ideal load method to achieve annual energy consumption, a recuperator efficiency (Siber DF Excellen 400 Plus) value of 0.85 was taken into account in terms of air renewal.

**Table 3.** Calculation of energy loads and demands of the four phases, using DesignBuilder.

Parameter		P1	P2	P3	P4
Total surface area	255.62 m <sup>2</sup>				
Total volume	703.8 m <sup>3</sup>				
Envelope airtightness ( <i>n</i> <sub>50</sub> )	ACH	1.05	0.95	0.75	0.59
Lighting load	kWh	1693.14	1693.14	1693.14	1693.14
Ventilation load (0.63 ACH)	kWh	982.85	984.18	985.79	988.86
Envelope infiltration load	kWh	1632.65	1435.93	1137.92	932.57
Occupancy load	kWh	1618.82	1616.98	1613.21	1610.34
Envelope <i>U</i> load	kWh	5103.92	5111.30	5126.22	5137.67
Windows <i>U</i> load	kWh	2302.07	2266.72	2315.77	2282.63
Annual energy demand due to infiltration	kWh/m <sup>2</sup> y	6.38	5.62	4.36	3.64
Total winter demand	kWh/y	5546.4	5433.30	5221.12	5040.88
Total winter energy demand	kWh/m <sup>2</sup> y	21.197	20.830	20.115	19.506
Total summer demand	kWh/y	4661.40	4555.62	4338.97	4150.43
Total summer energy demand	kWh/m <sup>2</sup> y	17.739	17.404	16.665	16.016
Solar gains through the glass in winter	kWh	−2701.90	−2701.90	−2701.90	−2701.90
Annual energy demand (DesignBuilder)	kWh/y	9983.60	9772.09	9401.70	9081.41
Total annual energy demand	kWh/m <sup>2</sup> y	28.367	27.659	26.210	24.957

**Figure 8.** DesignBuilder simulation model.

As can be observed, glazing solar gains lead to significant heating savings in winter, with a free gain of 10.57 kWh/m<sup>2</sup> y. This can occur thanks to the automated regulation system of opening and closing blinds or shutters depending on the solar radiation conditions and the *T<sub>i</sub>*, if allowed. In this way, the winter energy demand is 10.63 kWh/m<sup>2</sup> y in Phase 1 and 8936 kWh/m<sup>2</sup> y in Phase 4.

Table 4 shows the results obtained for the execution costs, maintenance costs, overall costs, annual energy savings due to infiltration reduction, and construction investment amortisation periods. These amortisation periods were estimated based on experiences

reported in other studies [63,64]. The databases of companies in the sector were used to calculate the installation costs. The cost of plastic adhesive jointing tape was based on a ratio of 30.59 EUR/mL, including the costs of the operating technicians. Elastic amorphous seals were valued according to previous experience and average construction company costs. The total considered cost, including labour, was 16.59 EUR/mL.

**Table 4.** Calculation of the investment amortisation period of the four phases.

Sealing Type	Cost (EUR/mL)	Measurement (mL)	Total Cost (EUR/m)	P1 (EUR)	P2 (EUR)	P3 (EUR)	P4 (EUR)
Hermetic liquid membrane	44.38	192.5	8542.80	8,542.81			
Expanding polyurethane foam	22.75	127.8	2907.45	2049.60	563.22	294.77	
Plastic adhesive joint tape	30.59	127.8	3909.36	2189.63	657.16	901.6	160.44
Elastic amorphous seals	16.59	111.7	1853.25	584.08	421.61	297.92	549.64
Initial investment costs	EUR		17,193.40	13,365.90	1641.99	1494.29	691.18
Maintenance costs (30 years)	EUR		2096	1437.0	325.0	237.0	97.2
Overall Cost ( $C_g$ )	EUR		19,289.4	14,802.9	1966.99	1731.29	788.38
Annual energy consumption	kWh/year			9983.60	9772.09	9401.70	9081.41
Annual savings (0.242 EUR/kWh)	EUR				51.74	155.61	244.90
Amortisation Period	Years				31.73	20.15	15.63

As can be observed, the amortisation periods of investments in the detection work and subsequent joinery sealing in the various phases were too long; they amounted to over 30 years for P2 and more than 15 years for P4. These values are well above those required for an adequate operation, which would be around 5–10 years. In addition, the electricity mix cost was higher in those years than in 2020, which would have led to even less favourable rates. A comparison of the four scenarios is shown in Figure 9.

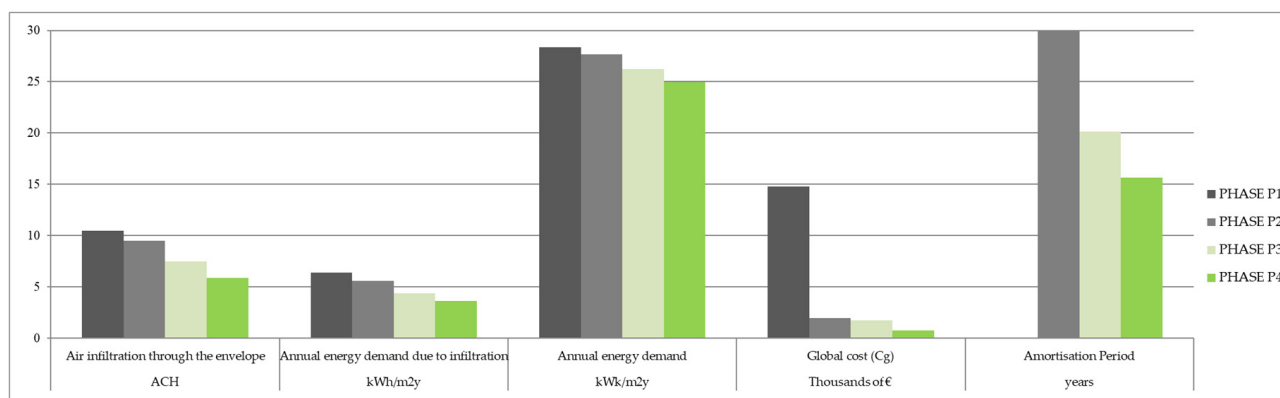


**Figure 9.** Results of the global cost for 30 years, energy due to infiltration, annual energy demand, and investment amortisation period in the four scenarios under study.

Lastly, we analysed the infiltration energy impact and investment amortisation in colder climate zones, in this case, in Central Europe [36,65], and compared the data with those of the Spanish Mediterranean region. To do this, we used the same case study, the house in Sitges, and simulated its location in Prague using DesignBuilder. The conditions of construction culture, execution costs, and per capita income, which do not differ substantially from those of Spain, support the validity of the comparison. The most notable difference was the electricity mix cost per kWh: it was EUR 0.3212 in Prague and EUR 0.242 in Sitges (Barcelona).

Table 5 and Figure 10 show the results obtained. One can see that the energy impact due to infiltration was around 217–228% higher than that of Sitges. The annual energy demand was 51,981 kWh/m<sup>2</sup> compared to 28,367 kWh/m<sup>2</sup> in Sitges, i.e., 183.25% higher. The PHS requirements would not be met in that case. On the other hand, the amortisation periods of the investments made to seal the envelopes, in all their phases, would be highly recommended, as they reduce the annual energy demand to a value of 46,087 kWh/m<sup>2</sup> y, allowing for amortisation of the investments in less than 5 years.

**Table 5.** Calculation of energy demand and investment amortisation period in Prague.

PRAGUE					
Parameter		P1	P2	P3	P4
Overall cost ( $C_g$ ) 94.1% per capita	EUR	13,929.5	1850.93	1629,14	741.87
Annual energy demand due to infiltration	kWh/y	−1153.89	−1045.44	−587.83	−651.70
Annual energy demand due to infiltration	kWh/m <sup>2</sup> y	13.84	12.72	10.93	8.33
Total winter energy demand	kWh/y	7035.30	6963.39	6813.58	6707.65
Total winter energy demand	kWh/m <sup>2</sup> y	46.43	44.99	43.27	40.82
Total summer energy demand	kWh/y	913.15	924.89	941.16	962.38
Total summer energy demand	kWh/m <sup>2</sup> y	5.555	5.430	5.339	5.270
Total annual energy demand	kWh/y	13,287.38	12,890.15	12,425.68	10,433.64
Total annual energy demand	kWh/m <sup>2</sup> y	51,981	50,427	48,610	46,087
Annual savings (0.3212 EUR/kWh)	EUR		127.56	276.72	916.44
Amortisation Period	Years		14.51	12.58	4.61

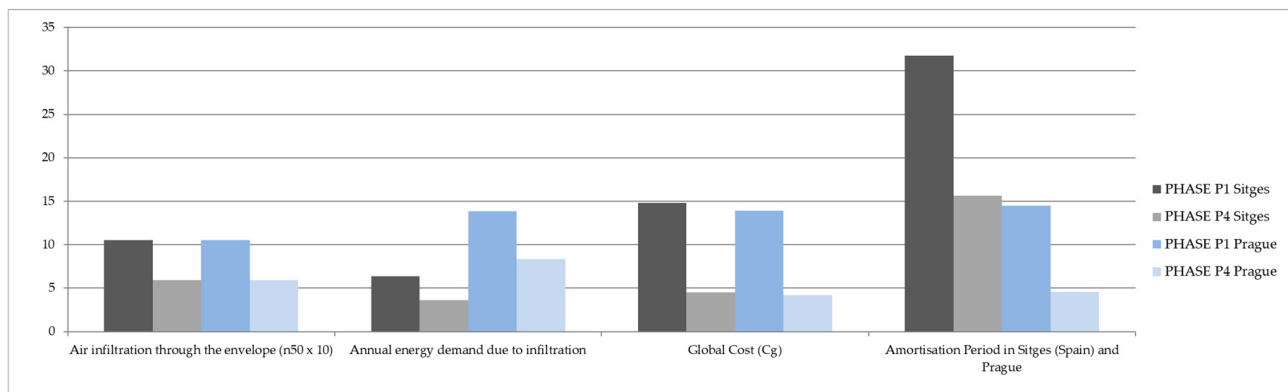


**Figure 10.** Comparative results of the global cost for 30 years, energy due to infiltration, annual energy demand, and investment amortisation period between P1 and P4 in Sitges and Prague.

## 5. Discussion

The application of the Passivhaus standard to housing on the Mediterranean coast has been the subject of ongoing debate. The most controversial factor is the overheating of the air and interior walls in summer, which leads to significant comfort loss and high air conditioning energy consumption.

Yet, to date, there has been little discussion on the need to build an envelope that would be as airtight as that required in Central Europe. As established by Wolfgang Feist, the current director of the Darmstadt Passivhaus Institut, and by Bo Adamson in the late 1980s, achieving an  $n_{50}$  value below 0.6 ACH seems to be an obvious condition to fulfil in that area. However, this requirement is not so justifiable on the Mediterranean coast, where the outside air rarely drops below 0 °C. It would therefore be relevant to conduct further



research and establish reasonable  $n_{50}$  value parameters taking into account construction execution costs and an amortisation period of less than 5 years for construction and sealing cost overruns. Another decisive factor in this issue is the market value that Passivhaus certification would give to the property in terms of capital gains. This variable would undoubtedly make it advisable to adopt  $n_{50}$  values below 0.6 ACH since the additional construction and sealing costs are usually much lower than the market value increase of the property.

It is also necessary to incorporate the variable of overall material implementation costs, which differ greatly from one country to another in the Mediterranean region and Central Europe. In Germany, they account for approximately 1600–2800 EUR/m<sup>2</sup>, while in Spain, they are in the range of 1400–2200 EUR/m<sup>2</sup>. Currently, the Passivhaus standard involves an additional cost that ranges from 3% to 8% of the total construction budget, with the average additional cost in Germany being 6%, though there have been cases where the extra cost is nil. In the Spanish Mediterranean area, the average cost overrun is around 27%, due to overall lower carpentry quality, poor airtightness, and the absence of heat recovery systems in conventional construction.

## 6. Conclusions

The requirement to apply a maximum value of  $n_{50}$  of 0.6 ACH in Passivhaus homes on the Spanish Mediterranean coast is subject to debate. Given the values found in this study for a PH house located in Sitges (Barcelona), it would seem more reasonable to apply the construction and sealing techniques of the Phase 1 envelope only. If successive phases of seal improvement were applied—P2, P3, and P4—to reduce the  $n_{50}$  value to 0.6 ACH with a higher material execution cost, the investment amortisation period would be too long, as it would range from 15 to 30 years. The resulting  $n_{50}$  value in P1 is 1.05, which is far above the PHS limit. However, the energy losses due to this value increase annual energy demand by only 13.66%, that is, 3.41 kWh/m<sup>2</sup> y, accounting for an annual energy cost increase of EUR 244.90. Compared to the execution costs of EUR 3827 for the three phases—the total costs applied in P4—the investment amortisation period would be over 15 years. The same would be true for phases F2 and F3, where the implementation costs would be EUR 1641.99 and EUR 3136.28, respectively, and the amortisation periods would be 31 years and 20 years. It would therefore be advisable not to undertake phases P2, P3, and P4. The property could not obtain the PHS with an  $n_{50}$  value of 1.05 ACH, but given that the PHS does not contribute to market value in the Spanish real estate valuation system, there is no need to continue improving envelope tightness with phases P2, P3, and P4.

When the same house is subjected to a DesignBuilder simulation in Prague, i.e., in a colder Central European climate, the scenario is entirely different. Severe winter conditions imply that reducing the air infiltration through the envelope to the  $n_{50}$  value of 0.59 ACH entails significant annual energy savings of 2853.74 kWh/y. The electricity mix costs EUR 0.324/kWh, and a substantial annual saving of EUR 916.44 is achieved. In this case, the amortisation period of the investments required to improve the construction is less than 5 years. We can thus conclude, in this specific case study, that the execution of phases P2, P3, and P4 would be feasible in cold continental climates, but in mild conditions, such as the Mediterranean climate, it would be more appropriate, in terms of energy and investments, to maintain the initial building construction solution of phase P1. To draw any concrete conclusions from an environmental perspective, it would first be necessary to conduct the arduous task of completing a whole life cycle assessment (LCA), including the P2, P3, and P4 sealing techniques.

To summarise, we are facing a complex problem that requires successive examinations and a detailed analysis of case studies in order to determine an  $n_{50}$  infiltration value adjusted to the climatic conditions and the energy and execution cost requirements according to each region or geographical area.

**Author Contributions:** Conceptualization, V.E.-I. and R.G.-V.; methodology, V.E.-I.; software, I.U.-B.; validation, V.E.-I., I.U.-B. and R.G.-V.; investigation, V.E.-I., I.U.-B. and R.G.-V.; resources, R.G.-V. and I.U.-B.; data curation, V.E.-I. and I.U.-B.; writing—original draft preparation, V.E.-I.; writing—review and editing, V.E.-I.; funding acquisition, R.G.-V. All authors have read and agreed to the published version of the manuscript.

**Funding:** This research received no external funding.

**Data Availability Statement:** There is not data available publicly.

**Acknowledgments:** The authors gratefully acknowledge the technical help provided by EVOWALL TECHNOLOGY S.L. and the RV4 architect's office in order to carry out the different tests needed for this paper.

**Conflicts of Interest:** The authors declare no conflicts of interest. The company and the architect's office had no role in the design of the study; in the collection, analyses, or interpretation of data; in the writing of the manuscript; or in the decision to publish the results.

## References

1. European Commission. Directive 2002/91/EC of the European Parliament and of the Council of 16 December 2002 on the energy performance of buildings. *Off. J. Eur. Commun.* **2003**, *L1*, 65–70.
2. European Commission. Directive 2010/31/EU of European Parliament and of the Council of 19 May 2010 on the energy performance of buildings (recast). *Off. J. Eur. Union* **2010**, *L153*, 13–35.
3. European Commission. Directive 2012/27/EU of European Parliament and of the Council of 25 October 2012 on energy efficiency, amending Directive 2009/125/EC and 2010/30/EU and repealing Directives 2004/8/EC and 2006/32/EC. *Off. J. Eur. Union* **2012**, *L315*, 1–56.
4. Attia, S.; Eleftheriou, P.; Xeni, F.; Morlot, R.; Ménézo, C.; Kostopoulos, V.; Betsi, M.; Kalaitzoglou, I.; Pagliano, L.; Cellura, M.; et al. Overview and future challenges of nearly zero energy buildings (nZEB) design in Southern Europe. *Energy Build.* **2017**, *155*, 439–458. [[CrossRef](#)]
5. Technical Building Code CTE. *Basic Document on Energy Savings DB-HE*; Spanish Ministry of Housing; Madrid, Spain, 2006. (In Spanish)
6. Spanish Ministry of Housing. *Orden VIV/984/2009, de 15 de Abril, Por la Que se Modifican Determinados Documentos Básicos del Código Técnico de la Edificación Aprobados por el Real Decreto 314/2006, de 17 de Marzo, y el Real Decreto 1371/2007, de 19 de Octubre*; Spanish Ministry of Housing; Madrid, Spain, 2009. (In Spanish)
7. Spanish Ministry of Public Works and Transport. *Orden FOM/1635/2013, de 10 de Septiembre, por la Que se Actualiza el Documento Básico DB-HE Ahorro de Energía, del Código Técnico de la Edificación, Aprobado por Real Decreto 314/2006, de 17 de Marzo; (Publicado en: «BOE» núm. 219, de 12 de Septiembre de 2013, Páginas 67137–67209)*; Spanish Ministry of Public Works and Transport; Madrid, Spain, 2013. (In Spanish)
8. Passive House—Passivhaus Institut (PHI). Available online: [https://passivehouse.com/02\\_informations/01\\_what\\_is\\_a\\_passive\\_house/01\\_what\\_is\\_a\\_passive\\_house.htm](https://passivehouse.com/02_informations/01_what_is_a_passive_house/01_what_is_a_passive_house.htm) (accessed on 9 April 2019).
9. Blázquez, T.; Suárez, R.; Ferrari, S.; Sendra, J. Improving winter thermal comfort in Mediterranean buildings upgrading the envelope: An adaptive assessment based on a real survey. *Energy Build.* **2023**, *278*, 112615. [[CrossRef](#)]
10. Reguis, A.; Tunzi, M.; Vand, B.; Tuohy, P.; Currie, J. Energy performance of Scottish public buildings and its impact on the ability to use low-temperature heat. *Energy Build.* **2023**, *290*, 113064. [[CrossRef](#)]
11. Liu, C.; Mohammadpourkarbasi, H.; Sharples, S. Evaluating the potential energy savings of retrofitting low-rise suburban dwellings towards the Passivhaus EnerPHit standard in a hot summer/cold winter region of China. *Energy Build.* **2021**, *231*, 110555. [[CrossRef](#)]
12. Lavafpour, Y.; Sharples, S.; Gething, B. The impact of building form on overheating control: A case study of Larch House. *Archit. Sci. Rev.* **2020**, *63*, 467–480. [[CrossRef](#)]
13. Bravo-Orlandini, C.; Gomez-Soberon, J.M.; Valderrama-Ulloa, C.; Sanhueza-Duran, F. Energy, Economic, and Environmental Performance of a Single-Family House in Chile Built to Passivhaus Standard. *Sustainability* **2021**, *13*, 1199. [[CrossRef](#)]
14. Causone, F.; Tatti, A.; Pietrobon, M.; Zanghirella, F.; Pagliano, L. Yearly operational performance of a nZEB in the Mediterranean climate. *Energy Build.* **2019**, *198*, 243–260. [[CrossRef](#)]
15. Strang, M.; Leardini, P.; Brambilla, A.; Gasparri, E. Mass Timber Envelopes in Passivhaus Buildings: Designing for Moisture Safety in Hot and Humid Australian Climates. *Buildings* **2021**, *11*, 478. [[CrossRef](#)]
16. Finegan, E.; Kelly, G.; O'Sullivan, G. Comparative analysis of Passivhaus simulated and measured overheating frequency in a typical dwelling in Ireland. *Build. Res. Inf.* **2020**, *48*, 681–699. [[CrossRef](#)]
17. Figueroa-Lopez, A.; Arias, A.; Oregi, X.; Rodriguez, I. Evaluation of passive strategies, natural ventilation and shading systems, to reduce overheating risk in a passive house tower in the north of Spain during the warm season. *J. Build. Eng.* **2021**, *43*, 102607. [[CrossRef](#)]
18. Jang, J.; Natarajan, S.; Lee, J.; Leigh, S.-B. Comparative Analysis of Overheating Risk for Typical Dwellings and Passivhaus in the UK. *Energies* **2022**, *15*, 3829. [[CrossRef](#)]

19. Chiesa, G.; Acquaviva, A.; Grosso, M.; Bottaccioli, L.; Florida, M.; Pristeri, E.; Sanna, E.M. Parametric Optimization of Window-to-Wall Ratio for Passive Buildings Adopting A Scripting Methodology to Dynamic-Energy Simulation. *Sustainability* **2019**, *11*, 3078. [[CrossRef](#)]
20. Hong, Y.; Ezech, C.I.; Deng, W.; Lu, J.; Ma, Y.; Jin, Y. Climate adaptation of design scheme for energy-conserving high-rise buildings—Comparative study of achieving building sustainability in different climate scenarios. *Energy Rep.* **2022**, *8*, 13735–13752. [[CrossRef](#)]
21. Brembilla, E.; Hopfe, C.J.; Mardaljevic, J.; Mylona, A.; Mantesi, E. Balancing daylight and overheating in low-energy design using CIBSE improved weather files. *Build. Serv. Eng. Res. Technol.* **2020**, *41*, 210–224. [[CrossRef](#)]
22. Rodriguez Vidal, I.; Otaegi, J.; Oregi, X. Thermal Comfort in NZEB Collective Housing in Northern Spain. *Sustainability* **2020**, *12*, 9630. [[CrossRef](#)]
23. Zune, M.; Tubelo, R.; Rodrigues, L.; Gillott, M. Improving building thermal performance through an integration of Passivhaus envelope and shading in a tropical climate. *Energy Build.* **2021**, *253*, 111521. [[CrossRef](#)]
24. Campo Ruano, P.; de Lapuerta Montoya, J.M.; Garcia-German, J.; Menendez Amigo, J.; Mendoza Alonso, V.; Camara Ruiz, I. Technical and constructive energy strategies of the first Passivhaus Plus school in Spain. *Inf. De La Constr.* **2023**, *75*, e492. [[CrossRef](#)]
25. Kang, Y.; Chang, V.W.-C.; Chen, D.; Graham, V.; Zhou, J. Performance gap in a multi-storey student accommodation complex built to Passivhaus standard. *Build. Environ.* **2021**, *194*, 107704. [[CrossRef](#)]
26. Escandón, R.; Calama-González, C.M.; Alonso, A.; Suárez, R.; León-Rodríguez, Á.L. How Do Different Methods for Generating Future Weather Data Affect Building Performance Simulations? A Comparative Analysis of Southern Europe. *Buildings* **2023**, *13*, 2385. [[CrossRef](#)]
27. Moreno-Rangel, A.; Sharpe, T.; McGill, G.; Musau, F. Indoor Air Quality and Thermal Environment Assessment of Scottish Homes with Different Building Fabrics. *Buildings* **2023**, *13*, 1518. [[CrossRef](#)]
28. Santin, O.G.; Grave, A.; Jiang, S.; Tweed, C.; Mohammadi, M. Monitoring the performance of a Passivhaus care home: Lessons for user-centric design. *J. Build. Eng.* **2021**, *43*, 102565. [[CrossRef](#)]
29. Mustafa, M.; Cook, M.J.; McLeod, R.S. Enhancing non-domestic Passivhaus auditoria ventilation design for improved indoor environmental quality. *Build. Environ.* **2023**, *234*, 110202. [[CrossRef](#)]
30. Otaegi, J.; Hernandez, R.J.; Oregi, X.; Martin-Garin, A.; Rodriguez-Vidal, I. Comparative Analysis of the Effect of the Evolution of Energy Saving Regulations on the Indoor Summer Comfort of Five Homes on the Coast of the Basque Country. *Buildings* **2022**, *12*, 1047. [[CrossRef](#)]
31. Liu, C.; Sharples, S.; Mohammadpourkarbasi, H. Evaluating Insulation, Glazing and Airtightness Options for Passivhaus EnerPHit Retrofitting of a Dwelling in China’s Hot Summer-Cold Winter Climate Region. *Energies* **2021**, *14*, 6950. [[CrossRef](#)]
32. Echarri-Iribarren, V.; Sotos-Solano, C.; Espinosa-Fernandez, A.; Prado-Govea, R. The Passivhaus Standard in the Spanish Mediterranean: Evaluation of a House’s Thermal Behaviour of Enclosures and Airtightness. *Sustainability* **2019**, *11*, 3732. [[CrossRef](#)]
33. Moreno-Rangel, A.; Sharpe, T.; McGill, G.; Musau, F. Indoor Air Quality in Passivhaus Dwellings: A Literature Review. *International. J. Environ. Res. Public Health* **2020**, *17*, 4749. [[CrossRef](#)]
34. Korsavi, S.S.; Jones, V.R.; Bilverstone, P.A.; Fuertes, A. A longitudinal assessment of the energy and carbon performance of a Passivhaus university building in the UK. *J. Build. Eng.* **2021**, *44*, 103353. [[CrossRef](#)]
35. Martinez-Soto, A.; Saldias-Lagos, Y.; Marincioni, V.; Nix, E. Affordable, Energy-Efficient Housing Design for Chile: Achieving Passivhaus Standard with the Chilean State Housing Subsidy. *Appl. Sci.* **2020**, *10*, 7390. [[CrossRef](#)]
36. Forde, J.; Hopfe, C.J.; McLeod, R.S.; Evins, R. Temporal optimization for affordable and resilient Passivhaus dwellings in the social housing sector. *Appl. Energy* **2020**, *261*, 114383. [[CrossRef](#)]
37. Feijó-Muñoz, J.; Poza-Casado, I.; González-Lezcano, R.; Pardal, C.; Echarri, V.; Fernández-Agüera, J.; Assiego de Larriva, R.; Fernández-Agüera, J.; Dios-Viéitez, M.J.; del Campo-Díaz, V.J.; et al. Methodology for the Study of the Envelope Airtightness of Residential Buildings in Spain: A Case Study. *Energies* **2018**, *11*, 704. [[CrossRef](#)]
38. Mitchell, R.; Natarajan, S. UK Passivhaus and the energy performance gap. *Energy Build.* **2020**, *224*, 110240. [[CrossRef](#)]
39. Rose, J.; Kragh, J.; Nielsen, K.F. Passive house renovation of a block of flats—Measured performance and energy signature analysis. *Energy Build.* **2022**, *256*, 111679. [[CrossRef](#)]
40. Yakimchuk, T.; Linhares, P.; Hermo, V. Evaluation of a modular construction system in accordance with the Passivhaus standard for components. *J. Build. Eng.* **2023**, *76*, 107234. [[CrossRef](#)]
41. Zhao, J.; Carter, K. Do passive houses need passive people? Evaluating the active occupancy of Passivhaus homes in the United Kingdom. *Energy Res. Soc. Sci.* **2020**, *64*, 101448. [[CrossRef](#)]
42. Echarri, V.; Espinosa, A.; Rizo, C. Thermal Transmission through Existing Building Enclosures: Destructive Monitoring in Intermediate Layers versus Non-Destructive Monitoring with Sensors on Surfaces. *Sensors* **2017**, *17*, 2848. [[CrossRef](#)] [[PubMed](#)]
43. Bienvenido-Huertas, D.; Moyano, J.; Rodríguez-Jiménez, C.E.; Marín, D. Applying an artificial neural network to assess thermal transmittance in walls by means of the thermometric method. *Appl. Energy* **2019**, *233–234*, 1–14. [[CrossRef](#)]
44. Xu, C.; Nielsen, P.V.; Liu, L.; Jensen, R.L.; Gong, G. Impacts of airflow interactions with thermal boundary layer on performance of personalized ventilation. *Build. Environ.* **2018**, *135*, 31–41. [[CrossRef](#)]

45. Poza-Casado, I.; Cardoso, V.E.; Almeida, R.M.; Meiss, A.; Ramos, N.M.; Padilla-Marcos, M. Residential buildings airtightness frameworks: A review on the main databases and setups in Europe and North America. *Build. Environ.* **2020**, *183*, 107221. [CrossRef]
46. Feijó-Muñoz, J.; Pardal, C.; Echarri, V.; Fernández-Agüera, J.; Assiego de Larriva, R.; Montesdeoca Calderín, M.; Poza-Casado, I.; Padilla-Marcos, M.A.; Meiss, A. Energy impact of the air infiltration in residential buildings in the Mediterranean area of Spain and the Canary Islands. *Energy Build.* **2019**, *188–189*, 226–238. [CrossRef]
47. Bienvenido-Huertas, D.; Fernández Quiñones, J.A.; Moyano, J.; Rodríguez-Jiménez, C.E. Patents Analysis of Thermal Bridges in Slab Fronts and Their Effect on Energy Demand. *Energies* **2018**, *11*, 2222. [CrossRef]
48. Echarri-Iribarren, V.; Rizo-Maestre, C.; Echarri-Iribarren, F. Healthy Climate and Energy Savings: Using Thermal Ceramic Panels and Solar Thermal Panels in Mediterranean Housing Blocks. *Energies* **2018**, *11*, 2707. [CrossRef]
49. Wang, Y.; Shi, S.; Zhou, Z.; Guo, S.; Zhao, B. Air infiltration rate distribution across Chinese five climate zones: A modelling study for rural residences. *Build. Environ.* **2024**, *252*, 111284. [CrossRef]
50. Porsani, G.B.; Casquero-Modreg, N.; Trueba, J.B.E.; Bandera, C.F. Empirical evaluation of EnergyPlus infiltration model for a case study in a high-rise residential building. *Energy Build.* **2023**, *296*, 113322. [CrossRef]
51. Poza-Casado, I.; Rodríguez-Del-Tío, P.; Fernández-Temprano, M.; Padilla-Marcos, M.; Meiss, A. An envelope airtightness predictive model for residential buildings in Spain. *Build. Environ.* **2022**, *223*, 109435. [CrossRef]
52. Younes, C.; Shdid, C.A.; Bitsuamlak, G. Air infiltration through building envelopes: A review. *J. Build. Phys.* **2012**, *35*, 267–302. [CrossRef]
53. Sherman, M.H. Estimation of infiltration from leakage and climate indicators. *Energy Build.* **1987**, *10*, 81–86. [CrossRef]
54. Benaddi, F.Z.; Boukhattem, L.; Tabares-Velasco, P.C. Multi-objective optimization of building envelope components based on economic, environmental, and thermal comfort criteria. *Energy Build.* **2024**, *305*, 113909. [CrossRef]
55. Aznar, F.; Echarri, V.; Rizo, C.; Rizo, R. Modelling the Thermal Behaviour of a Building Facade Using Deep Learning. *PLoS ONE* **2018**, *13*, e0207616. [CrossRef] [PubMed]
56. Liu, Z.; Zhou, X.; Tian, W.; Liu, X.; Yan, D. Impacts of uncertainty in building envelope thermal transmittance on heating/cooling demand in the urban context. *Energy Build.* **2022**, *273*, 112363. [CrossRef]
57. ISO 9869-1:2014; Thermal Insulation-Building Elements-In Situ Measurement of Thermal Resistance and Thermal Transmittance. Part 1: Heat Flow Meter Method. ISO: Geneva, Switzerland, 2014. Available online: <https://www.iso.org/standard/59697.html> (accessed on 13 April 2019).
58. Onatayo, D.; Aggarwal, R.; Srinivasan, R.S.; Shah, B. A data-driven approach to thermal transmittance (U-factor) calculation of double-glazed windows with or without inert gases between the panes. *Energy Build.* **2024**, *305*, 113907. [CrossRef]
59. Bucklin, O.; Müller, T.; Amtsberg, F.; Leistner, P.; Menges, A. Analysis of thermal Transmittance, air Permeability, and hygrothermal behavior of a solid timber building envelope. *Energy Build.* **2023**, *299*, 113629. [CrossRef]
60. UNE-EN 15459-1:2017; Energy Performance of Buildings—Economic Evaluation Procedure for Energy Systems in Buildings—Part 1: Calculation Procedures, Module M1-14. CEN. European Committee for Standardization: Brussels, Belgium, 2017. Available online: [https://standards.cen.eu/dyn/www/?p=204:110:0:::FSP\\_PROJECT,FSP\\_ORG\\_ID:40932,6209&cs=%20110690DD8F9BE238B61D722D035C11CAE](https://standards.cen.eu/dyn/www/?p=204:110:0:::FSP_PROJECT,FSP_ORG_ID:40932,6209&cs=%20110690DD8F9BE238B61D722D035C11CAE) (accessed on 11 June 2019).
61. IDAE. Informe de Precios Energéticos Regulados. April 2024. Available online: [https://www.idae.es/sites/default/files/estudios\\_informes\\_y\\_estadisticas/Tarifas\\_Reguladas\\_abril\\_2024.pdf](https://www.idae.es/sites/default/files/estudios_informes_y_estadisticas/Tarifas_Reguladas_abril_2024.pdf) (accessed on 7 May 2024).
62. Mihai, M.; Tanasiev, V.; Dinca, C.; Badea, A.; Vidu, R. Passive house analysis in terms of energy performance. *Energy Build.* **2017**, *144*, 74–86. [CrossRef]
63. Gainza-Barrencua, J.; Odriozola-Maritorena, M.; Hernandez\_Minguillon, R.; Gomez-Arriaran, I. Energy savings using sunspaces to preheat ventilation intake air: Experimental and simulation study. *J. Build. Eng.* **2021**, *40*, 102343. [CrossRef]
64. Echarri-Iribarren, V.; Rizo-Maestre, C.; Sanjuan-Palermo, J.L. Underfloor Heating Using Ceramic Thermal Panels and Solar Thermal Panels in Public Buildings in the Mediterranean: Energy Savings and Healthy Indoor Environment. *Appl. Sci.* **2019**, *9*, 2089. [CrossRef]
65. Dan, D.; Tanasa, C.; Stoian, V.; Brata, S.; Stoian, D.; Nagy Gyorgy, T.; Florut, S.C. Passive house design—An efficient solution for residential buildings in Romania. *Energy Sustain. Dev.* **2016**, *32*, 99–109. [CrossRef]

**Disclaimer/Publisher’s Note:** The statements, opinions and data contained in all publications are solely those of the individual author(s) and contributor(s) and not of MDPI and/or the editor(s). MDPI and/or the editor(s) disclaim responsibility for any injury to people or property resulting from any ideas, methods, instructions or products referred to in the content.